

Ante Skoblar
Teaching Assistant
University of Rijeka
Faculty of Engineering
Croatia

Roberto Žigulić
Full Professor
University of Rijeka
Faculty of Engineering
Croatia

Sanjin Braut
Full Professor
University of Rijeka
Faculty of Engineering
Croatia

Sebastijan Blažević
Teaching Assistant
University of Rijeka
Faculty of Engineering
Croatia

Dynamic Response to Harmonic Transverse Excitation of Cantilever Euler-Bernoulli Beam Carrying a Point Mass

In this paper, the calculation of the dynamic response to harmonic transverse excitation of cantilever Euler-Bernoulli beam carrying a point mass with the mode superposition method is presented. This method uses mode shapes and modal coordinate functions which are calculated by separation of variables and Laplace transformations. The accuracy of defined expressions is confirmed on examples with and without Rayleigh damping. All calculations are in good agreement with the results of commercial software based on finite element methods.

Keywords: dynamic response, Euler-Bernoulli beam, point mass, mode superposition method, Rayleigh damping.

1. INTRODUCTION

Dynamic analysis of a structure as continuum (where inertia, stiffness and damping are evenly distributed throughout the domain) has limited use in practice because of its mathematical complexity. However, the analysis of continuum systems, such as e.g. beam, gives us useful information of complete dynamic behaviour of more complex structures, so papers with different beam boundary conditions as [1], [2] and [3], beam excitations (in point [4], [5], base excitation [6], etc.) or beam materials (composite [7], [8], etc.) are published.

Transverse vibrations of uniform slender beam can be calculated using the Euler-Bernoulli theory. This paper describes specific combination of boundary conditions (cantilever beam with point mass) and excitation (harmonic excitation in one point) which can be found in practice as in [9] and [10] but this calculation procedure can be used for any boundary conditions.

In this paper, natural frequencies and mode shapes are calculated using the method of separation of variables and Laplace transformations of homogeneous part of differential equation of motion of cantilever beam carrying a point mass without damping. Then dynamic response of undamped and damped beam, where damping is defined with Rayleigh theory, is defined by the mode superposition method which uses mode shapes and modal coordinate functions. Calculation of modal coordinates functions is based on the orthogonality characteristic of mode shapes.

Analytical results, calculated by Matlab2010a on Windows 8, are compared to numerical results, calculated by software MSC.Nastran for Windows [11] where beam finite element, based on Timoshenko beam theory, is used for creation of finite element model.

2. DYNAMIC RESPONSE TO HARMONIC TRANSVERSE EXCITATION

Beam with the constant rectangular cross-section with point mass on position x_M and under the action of transversal harmonic force on position x_F is analysed.

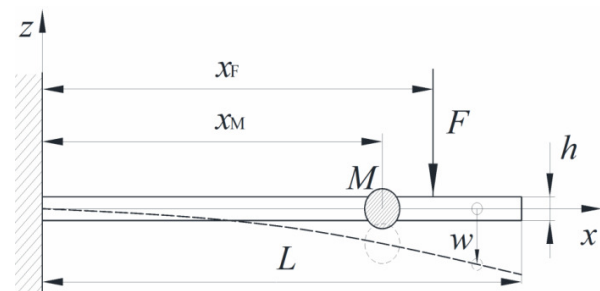


Figure 1. Sketch of cantilever Euler-Bernoulli beam carrying a point mass with harmonic transverse excitation in one point

A differential equation of forced vibrations of beam (see [12] and [13]) is defined by using the Hamilton's variational principle:

$$EI \frac{\partial^4 w}{\partial x^4} + EI \frac{c_d}{\omega^2} \frac{\partial^5 w}{\partial x^4 \partial t} + c \frac{\partial w}{\partial t} + \rho A \frac{\partial^2 w}{\partial t^2} + M \delta(x - x_M) \frac{\partial^2 w}{\partial t^2} = \hat{F} \sin(\Omega t) \delta(x - x_F) \quad (1)$$

where E is Young's modulus, I second moment of area, w transversal displacement, x beam longitudinal coordinate, c_d stiffness proportional and c mass proportional Rayleigh damping coefficient, ρ beam material density, A cross-section area, M value of point mass, x_M coordinate of point mass, \hat{F} excitation force amplitude and Ω angular frequency of harmonic excitation. Parts of (1) are flexural stiffness, inner damping, external damping [12] and inertia of beam, inertia of point mass and external force, respectively.

It is known that undamped linear dynamic systems have natural mode shapes, and that in every mode shape

Received: September 2016, Accepted: November 2016

Correspondence to: D. Sc. Ante Skoblar
Faculty of Engineering, University of Rijeka
Vukovarska 58, 51000 Rijeka, Croatia
E-mail: askoblar@riteh.hr

doi:10.5937/fmet1703367S

© Faculty of Mechanical Engineering, Belgrade. All rights reserved

FME Transactions (2017) 45, 367-373 367

different parts of the system are vibrating in phase, passing through equilibrium in the same moment. In the damped systems, however, this characteristic generally does not apply [14]. Rayleigh [12] has shown that there is a group of damped systems which have classical mode shapes. In this paper a Rayleigh definition of damping is used and uncoupled functions of modal coordinates are defined as a basic part of mode superposition method.

2.1 Natural frequencies and mode shapes

The objective of this chapter is to define natural frequencies and mode shapes from homogeneous part of differential equation of cantilever beam carrying a point mass without damping [2]:

$$EI \frac{\partial^4 w}{\partial x^4} + \rho A \frac{\partial^2 w}{\partial t^2} + M \frac{\partial^2 w}{\partial t^2} \delta(x - x_M) = 0. \quad (2)$$

Boundary conditions for cantilever beam are:

$$w(0, t) = w'(0, t) = w''(L, t) = w'''(L, t) = 0 \quad (3)$$

where ' is derivative with respect to x . Condition $w'''(L, t) = 0$ is valid if the free beam end is not loaded with external force or point mass. Differential equation (2) is solved by the method of separation of variables by which displacement is defined with the product of two separated functions of position and time:

$$w(x, t) = \psi(x) \sin(\omega t), \quad (4)$$

where $\psi(x)$ is mode shape and $\sin(\omega t)$ represents harmonic vibrations with angular natural frequency ω . After inclusion of (4) into (2) and division of the whole expression with $\sin(\omega t)$ an expression is obtained:

$$EI \psi^{IV} - \underbrace{(\rho A + M \delta(x - x_M))}_{\mathcal{E}(x)} \psi \omega^2 = 0, \quad (5)$$

where function $\mathcal{E}(x)$ is so called weighting function. Boundary conditions has to be satisfied after application of method of separation of variables which is possible if:

$$\psi(0) = \psi'(0) = \psi''(L) = \psi'''(L) = 0. \quad (6)$$

Equations (5) and (6) define eigenvalue problem which is solved by Laplace transformations with respect to x coordinate so equation (5) now has the form:

$$EI \cdot L(\psi^{IV}) - \rho A \cdot L(\psi) \omega^2 - M \omega^2 \cdot L(\psi \delta(x - x_M)) = 0 \quad (7)$$

Laplace transformation for function $\psi^{IV}(x)$ is:

$$L(\psi^{IV}(x)) = s^4 L(\psi(x)) - s^3 \psi(0) - s^2 \psi'(0) - s \psi''(0) - \psi'''(0) \quad (8)$$

where boundary conditions $\psi(0)$ and $\psi'(0)$ are equal to zero (see (6)), while Laplace transformation for equation part $\psi \delta(x - x_M)$ is:

$$L(\psi(x) \delta(x - x_M)) = e^{-sx_M} \psi(x_M). \quad (9)$$

After inclusion of (8) and (9) into (7) we obtain expression:

$$L(\psi(x)) = \psi''(0) \frac{s}{s^4 - k^4} + \psi'''(0) \frac{1}{s^4 - k^4} + \frac{M \omega^2 \psi(x_M) e^{-sx_M}}{EI (s^4 - k^4)}, \quad (10)$$

where wave number k is calculated from expression:

$$k = \left(\frac{\omega^2 \rho A}{EI} \right)^{0.25}. \quad (11)$$

Inverse Laplace follows:

$$\begin{aligned} \psi = & \psi''(0) \frac{\cosh(kx) - \cos(kx)}{2k^2} \\ & + \psi'''(0) \frac{\sinh(kx) - \sin(kx)}{2k^3} + \frac{M \omega^2 \psi(x_M)}{EI} \\ & \cdot U(x - x_M) \frac{\sinh(k(x - x_M)) - \sin(k(x - x_M))}{2k^3} \end{aligned} \quad (12)$$

and with the rest of the boundary conditions $\psi''(L) = \psi'''(L) = 0$ functions $\psi''(0)$ and $\psi'''(0)$ are calculated and mode shape function is defined as:

$$\begin{aligned} \psi(x) = & \frac{M \omega^2 \psi(x_M)}{4EI k^3} \left(A (\sin(kx) - \sinh(kx)) \right. \\ & - B (\cos(kx) - \cosh(kx)) - 2u(x - x_M) \\ & \cdot (\sin(kx - kx_M) - \sinh(kx - kx_M)) \left. \right) \end{aligned} \quad (13)$$

where values of A and B are calculated from expressions [9]:

$$A = 2 \frac{\left\{ \frac{\cos(kL - kx_M) + \cosh(kL - kx_M)}{\sin(kL) - \sinh(kL)} + \frac{\sin(kL - kx_M) + \sinh(kL - kx_M)}{\cos(kL) + \cosh(kL)} \right\}}{\left\{ \frac{\cos(kL) + \cosh(kL)}{\sin(kL) - \sinh(kL)} + \frac{\sin(kL) + \sinh(kL)}{\cos(kL) + \cosh(kL)} \right\}}, \quad (14)$$

$$B = \frac{\left\{ \begin{aligned} & \sin(kx_M) + \sinh(kx_M) \\ & + \cos(kL - kx_M) \sinh(kL) \\ & + \cosh(kL - kx_M) \sin(kL) \\ & - \sin(kL - kx_M) \cosh(kL) \\ & - \sinh(kL - kx_M) \cos(kL) \end{aligned} \right\}}{\cos(kL) \cosh(kL) + 1}. \quad (15)$$

By inserting condition $x = x_M$ in (13), the expression for calculation of natural frequencies ω is obtained:

$$\begin{aligned} M \omega^2 \left(2A (\sin(kx_M) - \sinh(kx_M)) \right. \\ \left. - B (\cos(kx_M) - \cosh(kx_M)) \right) - 4EI k^3 = 0 \end{aligned} \quad (16)$$

It is observed that equation (16) has the form $f(k)=0$ after inclusion of (11) so its zero points (see figure 2) define wave numbers k . Then natural frequencies from (11) and mode shapes from (13) can be obtained.

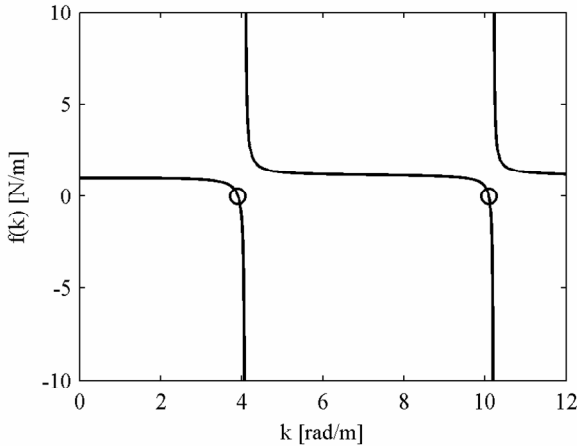


Figure 2. Zero points of equation (16)

The accuracy of calculated mode shapes are confirmed with (5).

2.2 Functions of modal coordinates

The equation (1) is solved by mode superposition method where the solution is assumed in form:

$$w(x,t) = \sum_{n=1}^{\infty} q_n(t) \psi_n(x) \quad (17)$$

where $q_n(t)$ are the functions of modal coordinates and $\psi_n(x)$ are the mode shapes (13). After inclusion of (17) into (1) and definition of stiffness proportional ($c_s = \beta \omega^2$) and mass proportional Rayleigh damping ($c = \alpha \varepsilon(x)$) [12], equation (1) has a form

$$EI \psi_i^{IV} q_i + EI \beta \psi_i^{IV} \dot{q}_i + \alpha \varepsilon(x) \psi_i \dot{q}_i + \varepsilon(x) \psi_i \ddot{q}_i = \hat{F} \sin(\Omega t) \delta(x - x_F) \quad (18)$$

Now, an orthogonality characteristic of normalized mode shapes is used to get uncoupled functions of modal coordinates. Normalized mass of mode shape is defined with expression:

$$M_i = \int_0^L \varepsilon(x) \psi_i^2(x) dx \quad (19)$$

and mass normalized mode shape can be determined from expression:

$$\bar{\psi}_i = \frac{\psi_i}{\sqrt{M_i}} \quad (20)$$

Mass normalized mode shape functions satisfy expressions:

$$\int_0^L \varepsilon(x) (\bar{\psi}_i(x))^2 dx = 1 \quad (21)$$

and

$$\int_0^L \varepsilon(x) \bar{\psi}_i(x) \bar{\psi}_j(x) dx = 0 \quad (22)$$

which makes them orthogonal with respect to the weighting function $\varepsilon(x)$. After inclusion of expression (5) into (18), multiplying expression (18) with mode shape function $\bar{\psi}_j$ and dividing it with the product of square roots of normalized masses ($\sqrt{M_i} \sqrt{M_j}$) an differential equation is obtained:

$$\begin{aligned} & \varepsilon(x) \omega_i^2 \bar{\psi}_i \bar{\psi}_j q_i + \beta \varepsilon(x) \omega_i^2 \bar{\psi}_i \bar{\psi}_j \dot{q}_i \\ & + \alpha \varepsilon(x) \bar{\psi}_i \bar{\psi}_j \dot{q}_i + \varepsilon(x) \bar{\psi}_i \bar{\psi}_j \ddot{q}_i = \\ & = \hat{F} \sin(\Omega t) \frac{\bar{\psi}_j(x_F)}{\sqrt{M_i}} \delta(x - x_F) \end{aligned} \quad (23)$$

After integration of eq. (23) over the beam domain for all mode shapes the following expression is obtained:

$$\begin{aligned} & \omega_i^2 q_i \int_0^L \varepsilon(x) \bar{\psi}_i \bar{\psi}_j dx + \beta \omega_i^2 \dot{q}_i \int_0^L \varepsilon(x) \bar{\psi}_i \bar{\psi}_j dx \\ & + \alpha \dot{q}_i \int_0^L \varepsilon(x) \bar{\psi}_i \bar{\psi}_j dx + \ddot{q}_i \int_0^L \varepsilon(x) \bar{\psi}_i \bar{\psi}_j dx = \\ & = \hat{F} \sin(\Omega t) \frac{\bar{\psi}_j(x_F)}{\sqrt{M_i}} \delta(x - x_F) \end{aligned} \quad (24)$$

where all combinations of indexes i and j of normalized mode shapes are under integral. Integrals in expression (24) with different indexes i and j are equal to zero while integrals with equal indexes $i=j$ are equal to one. As a result, a number of uncoupled expressions for functions of modal coordinates are given:

$$\begin{aligned} & \omega_i^2 q_i(t) + (\alpha + \beta \omega_i^2) \dot{q}_i(t) \\ & + \ddot{q}_i(t) = \hat{F} \sin(\Omega t) \frac{\bar{\psi}_i(x_F)}{\sqrt{M_i}} \end{aligned} \quad (25)$$

Furthermore, modal damping ratio ζ_i of i -th mode shape based on Rayleigh theory [12] is defined with:

$$\zeta = \frac{\alpha}{2\omega} + \frac{\beta\omega}{2} \quad (26)$$

so expression (25) has a new form:

$$\begin{aligned} & \omega_i^2 q_i(t) + 2\zeta_i \omega_i \dot{q}_i(t) \\ & + \ddot{q}_i(t) = \hat{F} \sin(\Omega t) \frac{\bar{\psi}_i(x_F)}{\sqrt{M_i}} \end{aligned} \quad (27)$$

with a solution:

$$\begin{aligned} q_i(t) = & e^{-\zeta_i \omega_i t} \left[\frac{\dot{q}_{i0} + \zeta_i \omega_i q_{i0}}{\omega_i} \sin(\omega_i t) \right. \\ & + q_{i0} \cos(\omega_i t) + \frac{\bar{\psi}_i(x_F) \hat{F}}{\omega_i \sqrt{M_i}} \\ & \left. \cdot \int_0^t \sin(\Omega \tau) e^{\zeta_i \omega_i \tau} \sin(\omega_i(t - \tau)) d\tau \right] \end{aligned} \quad (28)$$

where $\omega_i' = \omega_i \sqrt{1 - \zeta_i^2}$ is natural damped frequency of i -th mode shape.

3. EXAMPLE 1

In this example, natural frequencies and mode shapes for a beam which can be modelled by Euler-Bernoulli theory are verified by Nastran. Also, numerical overflow which appears at higher natural frequencies is analysed.

Beam dimensions are 0.46m*0.03m*0.0007m and beam material is galvanized steel with Young's modulus $E=2.1 \cdot 10^{11}$ Pa, the density $\rho=7780$ kg/m³ and the Poisson's coefficient $\nu=0.3$.

The accuracy of the analytical results will be confirmed using the software Nastran [11] by comparison of natural frequencies and mode shapes. Beam finite elements with two nodes and unconnected finite element degrees of freedom T_y (displacement parallel to x axis) and R_z (rotation parallel to z axis, see figure 1) and an option of coupled mass are used. After confirmation of convergence of the results, 50 finite elements of the same size is used for modelling of the beam which gives, approximately, 10 finite elements along one mode shape peak of the highest mode shape. Point mass with 0.01 kg is positioned at 36. node (on coordinate $x=0.32$ m) and natural frequencies are calculated. In table 1, a good agreement between analytical results calculated from zero points of equation (16) and expression (11) (see figure 2) and Nastran results can be seen.

Table 1. Natural frequencies

Natural frequency No.	Analytic expressions, Hz	Nastran, Hz
1.	2.55	2.55
2.	17.01	17.01
3.	44.65	44.65
4.	92.85	92.85
5.	156.25	156.24
6.	217.88	217.86

In figures 3 and 4 a good agreement between mode shapes calculated with (13) and (29) and with Nastran can be seen.

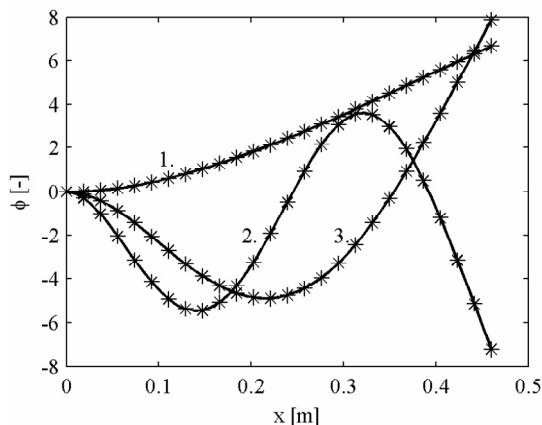


Figure 3. Mode shapes 1-3. calculated with expressions (13) and (29) (—) and with Nastran (*).

The described approach gives exact natural frequencies and mode shapes for 1-st to 5-th mode shape, but the error is observed for 6-th and higher mode shapes. The values of equation (16) whose zero points give natural frequencies start to oscillate (see figure 5) which grows for higher natural frequencies. This error is caused by a numerical overflow [9] which appears in expressions (14) and (15) because hyperbolic functions with high values are in ratios.

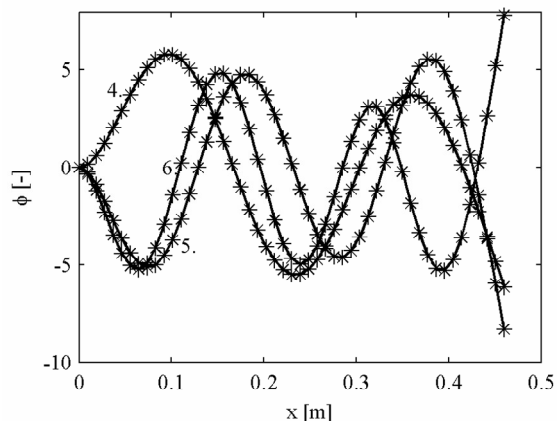


Figure 4. Mode shapes 4-6. calculated with expressions (13) and (29) (—) and with Nastran (*).

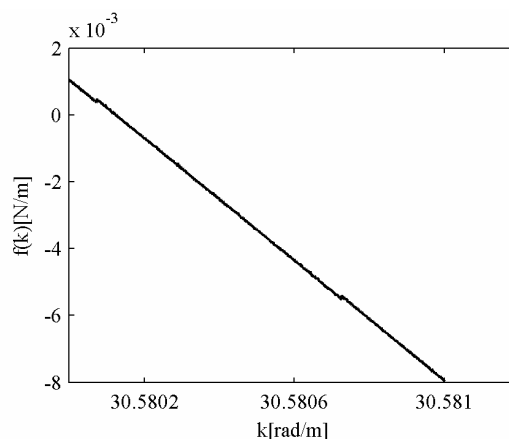


Figure 5. Value of function (16) around zero point of 5-th natural frequency

As a result a group of incorrect natural frequencies can be calculated in the vicinity of the exact natural frequency (see figure 6).

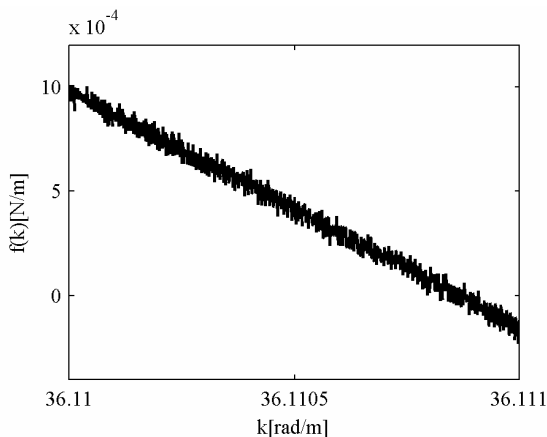


Figure 6. Value of function (16) around zero point for 6-th natural frequency

Furthermore, it was shown that with reduction of the point mass the natural frequency of the beam with point mass converge toward natural frequency of beam without mass (see table 2).

Table 2. Values of natural frequencies with reduction of point mass

Natural frequency No.	Natural frequencies of beam with point mass, Hz			Beam natural freq., Hz
	0.01 kg	0.001kg	0.0001kg	
1.	2.55	2.75	2.77	2.78
2.	17.01	17.35	17.39	17.4
3.	44.65	48.18	48.66	48.72
4.	92.85	95.09	95.43	95.47
5.	156.25	157.61	157.8	157.81
6.	217.88	233.04	235.47	235.73

4. EXAMPLE 2

The objective of example 2 is the comparison of numerical and analytical results of equation (27) i.e. the function of modal coordinates and comparison of dynamic response without damping calculated by mode superposition method and by direct transient method with Nastran [11].

The harmonic transversal force have the amplitude 1 N and frequency of 45 Hz which is more than four times lower than the highest calculated 6-th natural frequency (217 Hz) in order to get more accurate results [9]. Force is acting at 23. node (on coordinate $x=0.2$ m). Good agreement of results for function of modal coordinate can be seen on figure 7 which confirms the accuracy of analytic solution.

An overflow also occurs in the function of modal coordinates but it can be avoided by the procedure explained in [9].

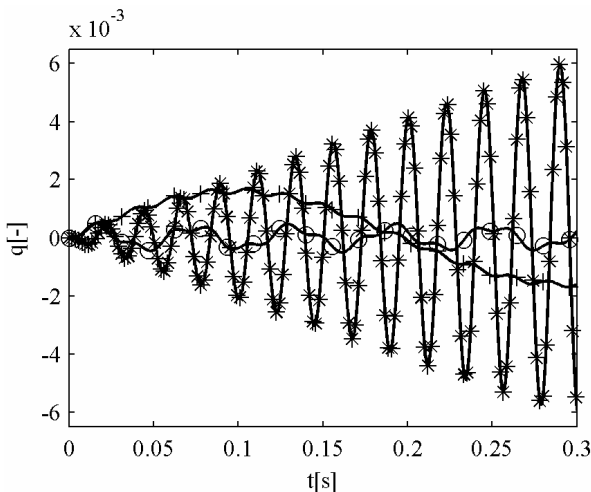


Figure 7. Comparison of 1.(+), 2.(o) and 3.(*) function of modal coordinates calculated by numerical solution of differential equation (27) and by expression (28) (—)

In this example beam dynamic response in node 46. (at coordinate $x=0.41$ m) is also calculated using mode superposition method and by direct transient method in Nastran [11] and calculated results are in good agreement which can be seen on figure 8. Function of modal coordinate for 3. mode shape have largest

influence on response because its frequency (44.65 Hz) is close to excitation frequency (45 Hz).

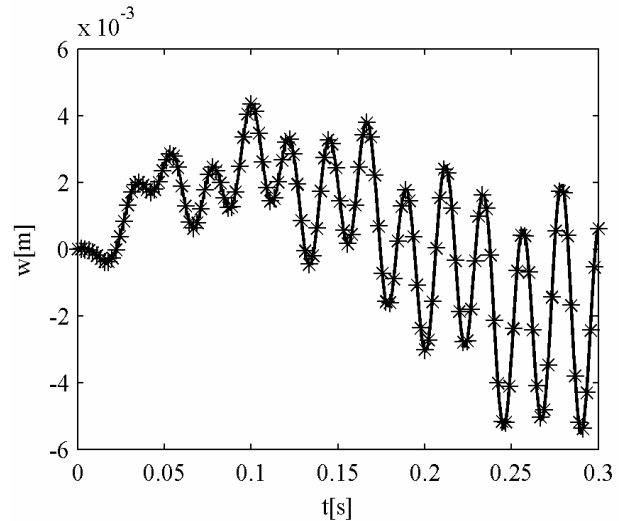


Figure 8. Dynamic response of undamped beam at node 46. calculated with expression (17) (—) and with software Nastran (*)

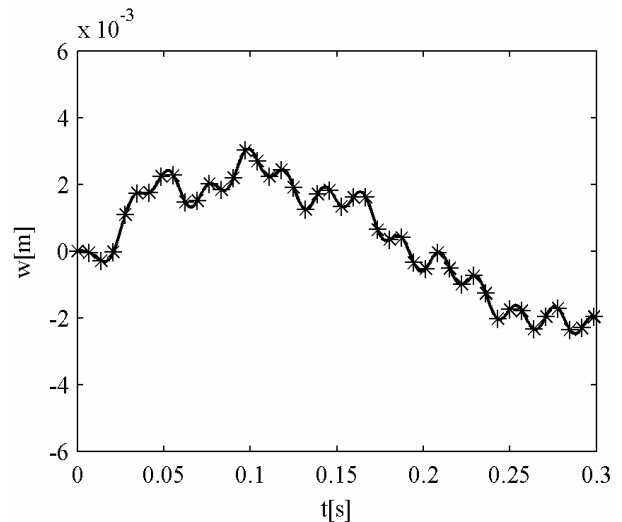


Figure 9. Dynamic response of damped beam calculated with mode superposition method (—) and with Nastran(*)

5. EXAMPLE 3

The objective of example 3 is the comparison of results of dynamic response for damped beam by using mode superposition method with results of software Nastran.

Overall structural damping coefficient G is used in Nastran for definition of damping in direct transient method. Structural damping is connected with displacement and it has constant value e.g. it does not depend up on frequency. In presented theory of mode superposition method we use Rayleigh damping which depends up on frequency. With the aim of comparing analytic results with Nastran, we will use the equivalent viscous damping to define G . Equivalent viscous damping grows linearly with the frequency and it can be equal with Rayleigh damping if Rayleigh mass proportional coefficient is equal to zero. In that case overall structural coefficient G can be calculated from the value of Rayleigh stiffness proportional coefficient

(e.g. $\beta=0.001$ in this example) and first natural angular frequency ω_1 [11] from expression:

$$G = 2\xi_i = \beta\omega_1. \quad (29)$$

The setup parameters in direct transient analysis in Nastran are $f_1=W/3=2.5492$ Hz and $G=0.016$. At figure 9 an transversal dynamic response at node 46. can be seen.

6. CONCLUSION

In this paper an analytic expression for dynamic response to transverse harmonic force of Euler-Bernoulli cantilever beam with the point mass is defined. A procedure for defining natural frequencies, mode shapes and functions of modal coordinates is described and results are used in the modal superposition method.

Expressions for natural frequencies are tested by reducing the point mass, whereby natural frequencies converged toward natural frequencies of cantilever beam without point mass, which is a confirmation of expressions accuracy. During the analysis of natural frequencies it is observed that error occurs when higher natural frequencies are calculated. Errors are caused by numerical overflow which appears because hyperbolic functions with high values are in ratios.

In this paper damping is defined with Rayleigh's theory whereby it is possible to calculate uncoupled functions of modal coordinates, which is described in detail. For confirmation of the results a software based on finite element method was used (Nastran). Structural damping for the direct transient method in Nastran was defined from equivalent viscous damping which correspond to Rayleigh stiffness proportional damping while mass proportional damping was set to zero. All calculated results are in good agreement.

ACKNOWLEDGMENT

AdriaHub is a collaborative project funded by the European Union (EU) inside the Adriatic IPA CBC Programme, an Instrument for the Pre-Accession Assistance (IPA) of neighbouring countries of the Western Balkans, thanks to the investments in Cross-Border Cooperation (CBC) aiming at joint economic and social development. Details in Savoia et al. [15].

This study is also supported by University of Rijeka Grants (No. 13.09.1.2.11 and No. 13.09.2.2.19).

REFERENCES

- [1] Han SM, Benaroya H and Wei T. Dynamics of transversely vibrating beams using four engineering theories. *J Sound Vibrat*, 225, pp. 935–988, 1999.
- [2] Chen, Y.: On the vibration of beams or rods carrying a concentrated mass. *J Appl Mech*, 30, pp. 310–311, 1963.
- [3] Geist, B.: The Effect of Structural Damping on Nodes for the Euler-Bernoulli Beam: A Specific Case Study, *Appl. Math. Lett.*, Vol. 7, No. 3, pp. 51-55, 1994.
- [4] Piccardo, G., Tubino, F.: Dynamic Response of Euler-Bernoulli beams to Resonant Harmonic Moving Loads, *Structural Engineering and Mechanics*, Vol. 44, No. 5, pp. 681-704, 2012.
- [5] Hamdan, M.N. et al.: Force and Forced Vibrations of a Restrained Cantilever Beam Carrying a Concentrated Mass, *Eng. Sci.*, Vol. 3, pp. 71-83, 1991.
- [6] Erturk, A., Inman, D.J.: On Mechanical modeling of Cantilevered Piezoelectric Vibration Energy Harvesters, *Journal of Intelligent Material Systems and Structures*, Vol. 19, p.p. 1311-1325, 2008.
- [7] Živković, I., Pavlović, A., Fragassa, C.: Improvements in Wood Thermoplastic Matrix Composite Materials Properties by Physical and Chemical Treatments, *Int J Qual Res*, Vol. 10, No. 3, pp. 205-218, 2016.
- [8] Saghafi, H., Brugo, T.M., Zucchelli, A., Fragassa, C., Minak, G.: Comparison of the Effect of Preload and Curvature of Composite Laminate under Impact Loading, *FME Transactions*, Vol. 44, No. 4, p.p. 353-357, 2016.
- [9] Skoblar, A., Žigulić, R., Braut, S.: Numerical Ill-conditioning in evaluation of the dynamic response of structures with mode superposition method, *Proc IMechE Part C: J Mechanical Engineering Science*, in press, DOI: 10.1177/0954406216653982, 2016.
- [10] Pavlović, A., Fragassa, C.: Analysis of Flexible Barriers Used as Safety Protection in Wood-working, *Int J Qual Res*, Vol. 10, No. 1, pp. 71-88, 2016.
- [11] MSC. Nastran Version 68. Basic dynamic analysis user's guide. MSC. Software Corporation, 2004.
- [12] Banks, H.T., Inman, D.J.: On damping mechanisms in beams, *Journal of Applied Mechanics*, Vol. 58, pp. 716-723, 1991.
- [13] Goel, R.P.: Vibrations of a Beam Carrying a Concentrated Mass, *Journal of Applied Mechanics*, pp. 821-822, September 1973.
- [14] Caughey, T.K., O'Kelly, M.E.J.: Classical Normal Modes in Damped Linear Dynamic Systems, *J. Applied Mechanics*, p.p. 583-588, September 1965.
- [15] Savoia, M., Stefanovic, M. and Fragassa, C.: Merging technical competences and human resources with the aim at contributing to transform the Adriatic area in a stable hub for a sustainable technological development, *Int J Qual Res*, 10, pp. 1–12, 2016.

ДИНАМИЧКИ ОДГОВОР НА ХАРМОНИЧНУ ПОПРЕЧНУ ПОБУДУ КОНЗОЛЕ EULER-BERNOULLI SA KONCENTRICHNIM MASAMA

A. Скоблар, P. Жигулић, С. Браут, С. Блажевић

У овом раду приказан је прорачун динамичког одговора на хармоничну попречну побуду конзоле Euler-Bernoulli са концентричним масама, методом режима суперпозиције. Метод суперпозиције користи режиме облика и координата функције које су изра-

чунате одвајањем променљивих и Лаплас трансформацијама. Тачност дефинисаних израза су потврђени на примерима са и без Raleigh пригушења. Сви резу-

лтати су у сагласности са резултатима комерцијалних софтвера на основу метода коначних елемената.